

Eulerian semiclassical computational methods in quantum dynamics

Shi Jin

Department of Mathematics
University of Wisconsin-Madison

outline

- **Classical mechanics**: Hamiltonian system, discontinuous Hamiltonian, transmission and reflection (J-Wen)
- **Quantum barriers**: quantum-classical coupling, interference (J-Novak)
- **Diffraction**: use GTD (J-Yin)
- **Surface hopping** (J-Qi-Zhang)
- **Gaussian beam method** (J-Wu-Yang)
- conclusion

I: Classical Mechanics for singular Hamiltonians

- a Hamiltonian system:

$$d\mathbf{x}/dt = \nabla_{\xi} H$$

$$d\xi/dt = -\nabla_{\mathbf{x}} H$$

$H=H(\mathbf{x}, \xi)$ is the **Hamiltonian**

Classical mechanics: $H=1/2 |\xi|^2+V(\mathbf{x})$ (\Rightarrow **Newton's second law**)

Geometrical optics: $H = c(\mathbf{x}) |\xi|$

computational method based on solving the Hamiltonian system is referred to as the particle method, or a **Lagrangian** method

- Phase space representation:

$$f_t + \nabla_{\xi} H \cdot \nabla_{\mathbf{x}} f - \nabla_{\mathbf{x}} H \cdot \nabla_{\xi} f = 0$$

$f(t, \mathbf{x}, \xi)$ is the density distribution of a classical particle at position \mathbf{x} , time t , with momentum ξ

Computational methods based on solving the Liouville equation will be referred to as the **Eulerian** method

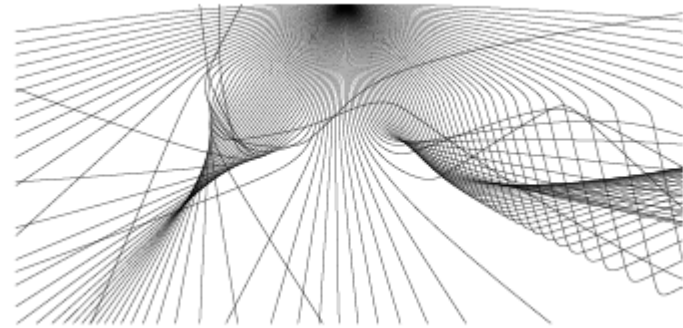
The Liouville equation can be solved by **method of characteristics** if H is smooth

Lagrangian vs Eulerian

- **Lagrangian:** simple, efficient in high dimension
particles (rays) may diverge: loss of accuracy, remeshing (increasing particles) is needed which may be complicated
- **Eulerian:** solving PDEs on a fixed mesh--
high order accuracy; computational cost higher (reducing cost: moment closure, level set method)

A ray tracing result

- Rays or particles may diverge, so it becomes highly inaccurate to reconstruct quantities of interests: fields (electric or electromagnetic, Bohm potential, etc)
- Figure by O. Runborg



Discontinuous Hamiltonians

- $H=1/2|\xi|^2+V(x)$: $V(x)$ is **discontinuous**- potential barrier,
- $H=c(x)|\xi|$: $c(x)$ is **discontinuous**-different index of refraction
- quantum tunneling effect, semiconductor device modeling, plasmas, geometric optics, interfaces between different materials, etc.
- Modern theory (KAM theory) and numerical methods (symplectic scheme) for Hamiltonian system all assume **smooth** Hamiltonian

Analytic issues

$$f_t + \nabla_{\xi} H \cdot \nabla_{\mathbf{x}} f - \nabla_{\mathbf{x}} H \cdot \nabla_{\xi} f = 0$$

- The PDE does not make sense for discontinuous H .
What is a weak solution?

$$d\mathbf{x}/dt = \nabla_{\xi} H$$

$$d\xi/dt = -\nabla_{\mathbf{x}} H$$

- How to define a solution of systems of ODEs when the RHS is discontinuous or/and measure-valued? (DiPerna-Lions-Ambrosio renormalized solution does not apply here—only work for BV RHS)

How do we extend the mathematical theory
to singular Hamiltonian system

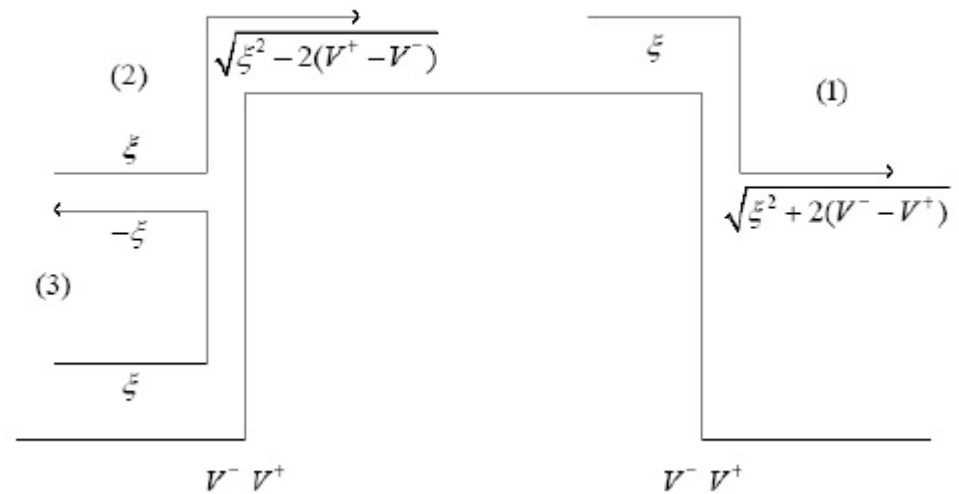
Our approach: build in correct
physics at the singularity:
transmission, reflection, diffraction,
quantum tunneling, surface
hopping, ...

Classical particles at barriers

Particles either transmit or reflect

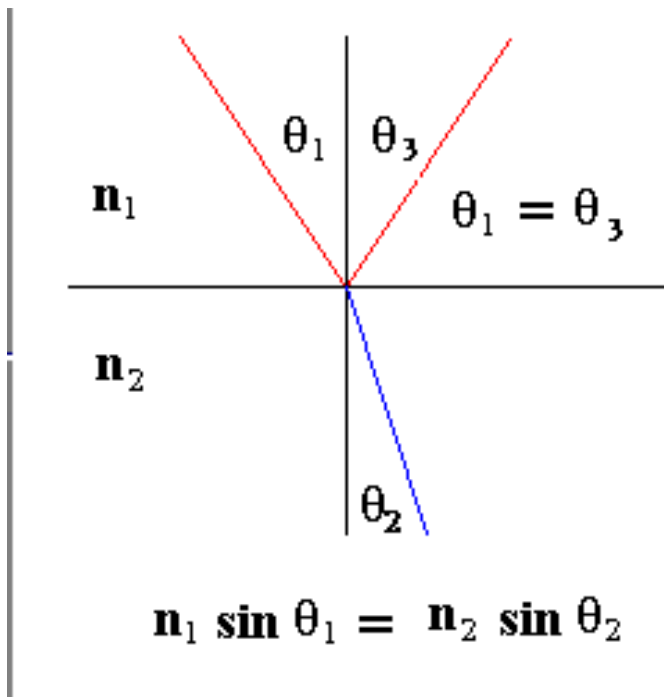
Hamiltonian is conserved:

$$H^+ = H^-$$

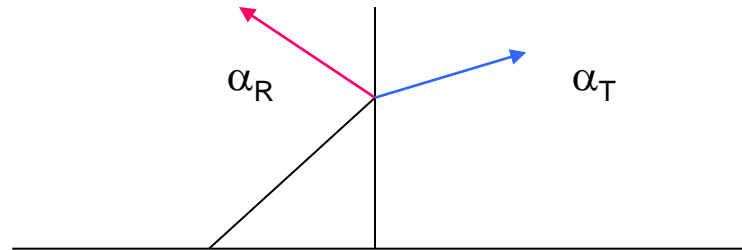


Snell-Descartes Law of refraction

- When a plane wave hits the interface, $H=c|\xi|$ is conserved: the angles of incident and transmitted waves satisfy ($n=c_0/c$)



Solution to Hamiltonian System with discontinuous Hamiltonians



- Particles cross over or be reflected by the corresponding transmission or reflection coefficients (probability)
- Based on this definition we have also developed **particle methods** (both deterministic and Monte Carlo) methods

Eulerian picture: An interface condition

an **interface condition** for f should be used to connect
(the good) Liouville equations on both sides of the interface.

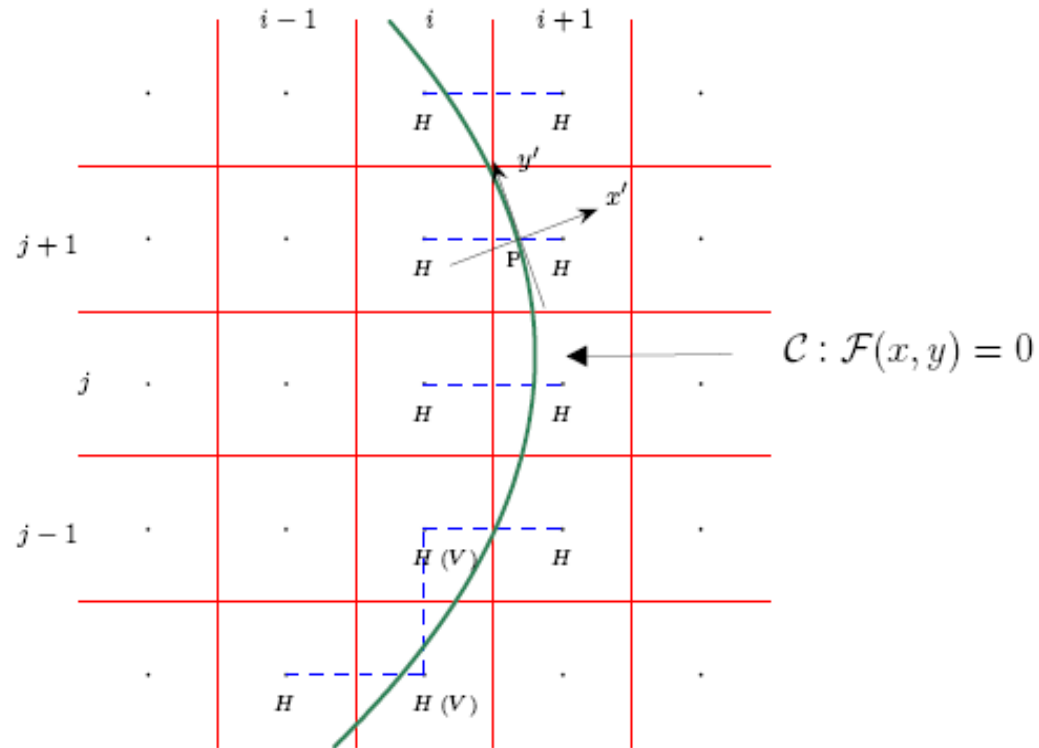
$$f(x^+, \xi^+) = \alpha_T f(x^-, \xi^-) + \alpha_R f(x^+, -\xi^+) \quad \text{for } \xi^+ > 0$$
$$H(x^+, \xi^+) = H(x^-, \xi^-)$$

α_R : reflection rate α_T : transmission rate

$$\alpha_R + \alpha_T = 1$$

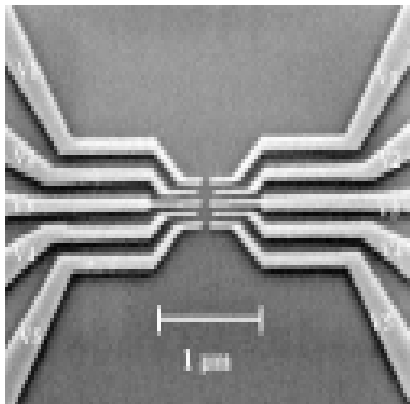
- α_T, α_R defined from the original “microscopic” problems
- This gives a mathematically **well-posed** problem that is **physically relevant**
- We can show the interface condition is **equivalent to Snell’s law** in geometrical optics
- **A new method of characteristics** (bifurcate at interfaces)

Curved interface



II. Quantum barrier: a multiscale approach (with *K. Novak*, MMS, JCP)

We want to study quantum scale phenomena using a largely classical scale model.



- Nanotechnology
- Electron transport in semiconductors
- Tunneling diodes
- Quantum dot structures
- Quantum computing

A quantum-classical coupling approach for thin barriers

- Barrier width in the order of De Broglie length, separated by order one distance
- Solve a time-independent Schrodinger equation for the local barrier/well to determine the scattering data
- Solve the classical liouville equation elsewhere, using the scattering data at the interface

A step potential ($V(x)=1/2 H(x)$)

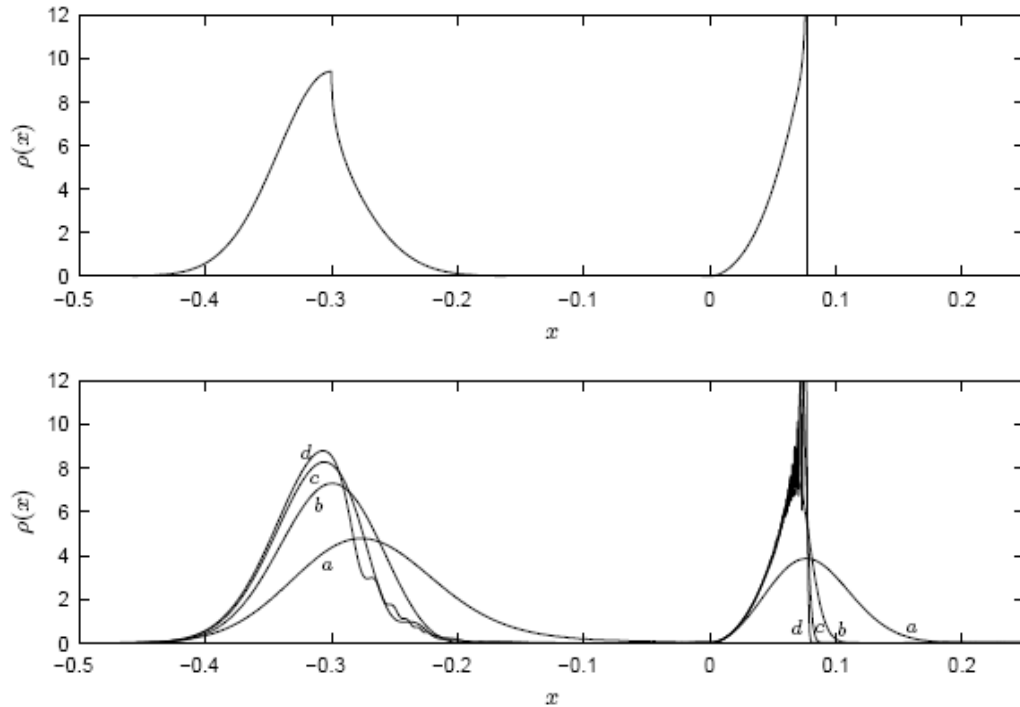


FIG. 5.1. Position densities for the semiclassical Liouville (top) and Schrödinger (bottom) solutions of Example 5.1. The Schrödinger solution shows $\epsilon = (a) 200^{-1}$, $(b) 800^{-1}$, $(c) 3200^{-1}$ and $(d) 12800^{-1}$. The position density of Liouville solution exhibits a caustic near $x = 0.08$ and the peak is unbounded. For the Schrödinger solution the peak reaches a height of 19 for the $\epsilon = 12800^{-1}$. The plots are truncated for clarity.

Resonant tunnelling

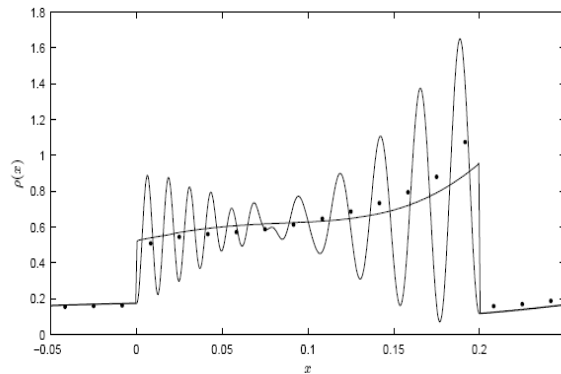
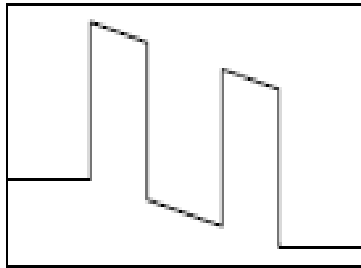


FIG. 5.4. Detail of Fig. 5.3 showing position densities for the numerical semiclassical Liouville and von Neumann solutions. The \bullet shows the numerical solution for with 150 grid points over the domain $[-1.25, 1.25]$. The solid line shows the "exact" Liouville solution and the von Neumann solution using $\varepsilon = 0.002$.

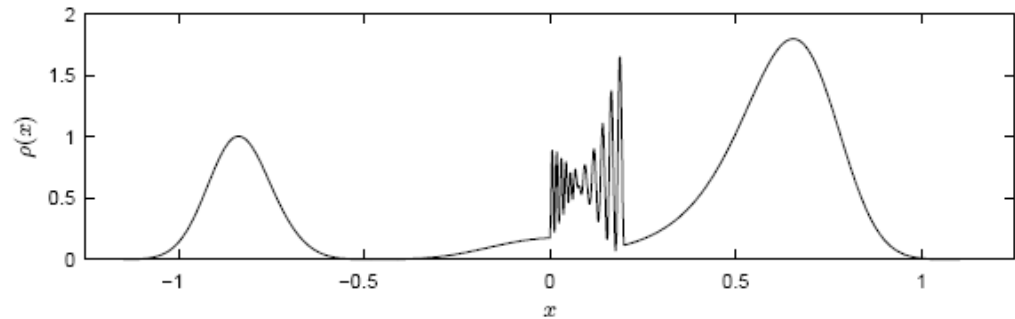
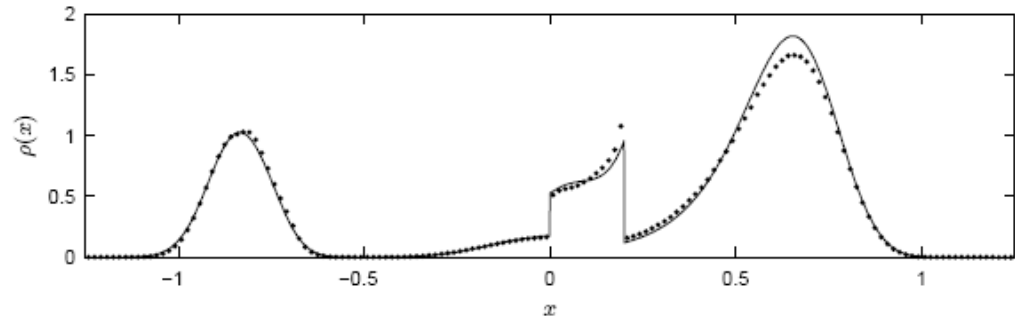
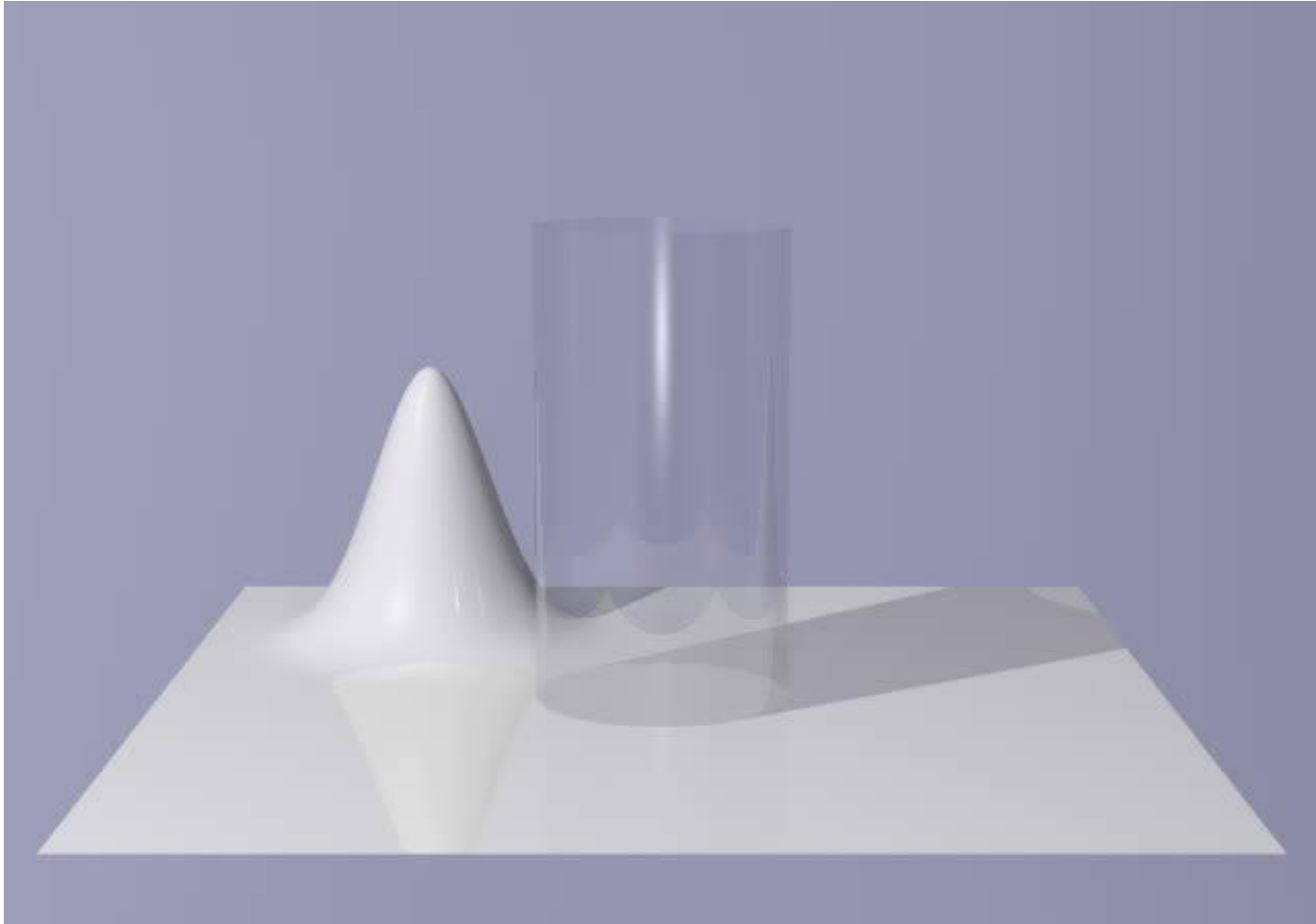
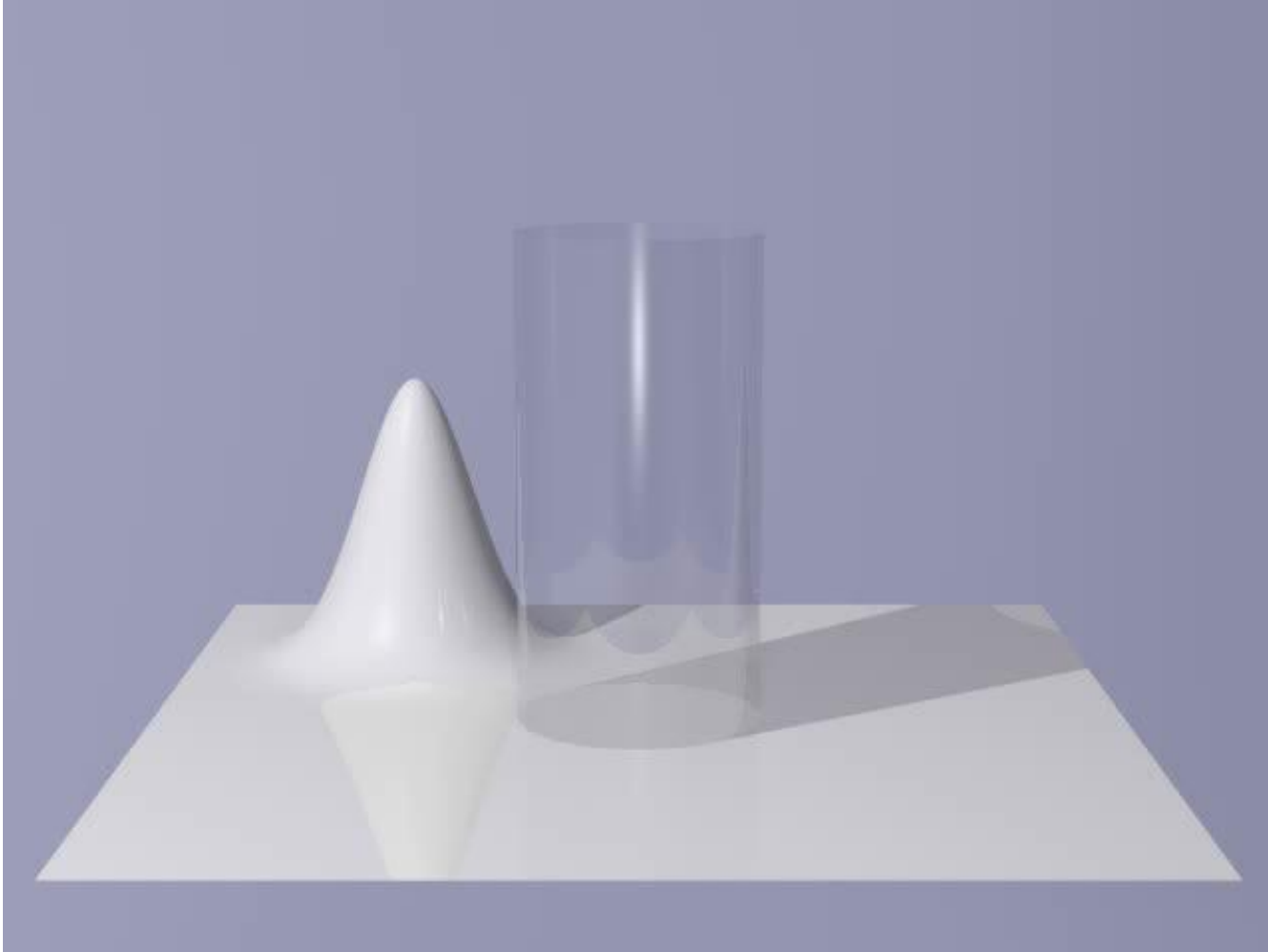


FIG. 5.3. Position densities for the numerical semiclassical Liouville (top) and von Neumann (bottom) solutions of Example 5.3. The \bullet in the Liouville plot shows the numerical solution for with 150 grid points over the domain $[-1.25, 1.25]$. The solid line shows the numerical solution for 3200 grid points. The von Neumann solution is for $\varepsilon = 0.002$.

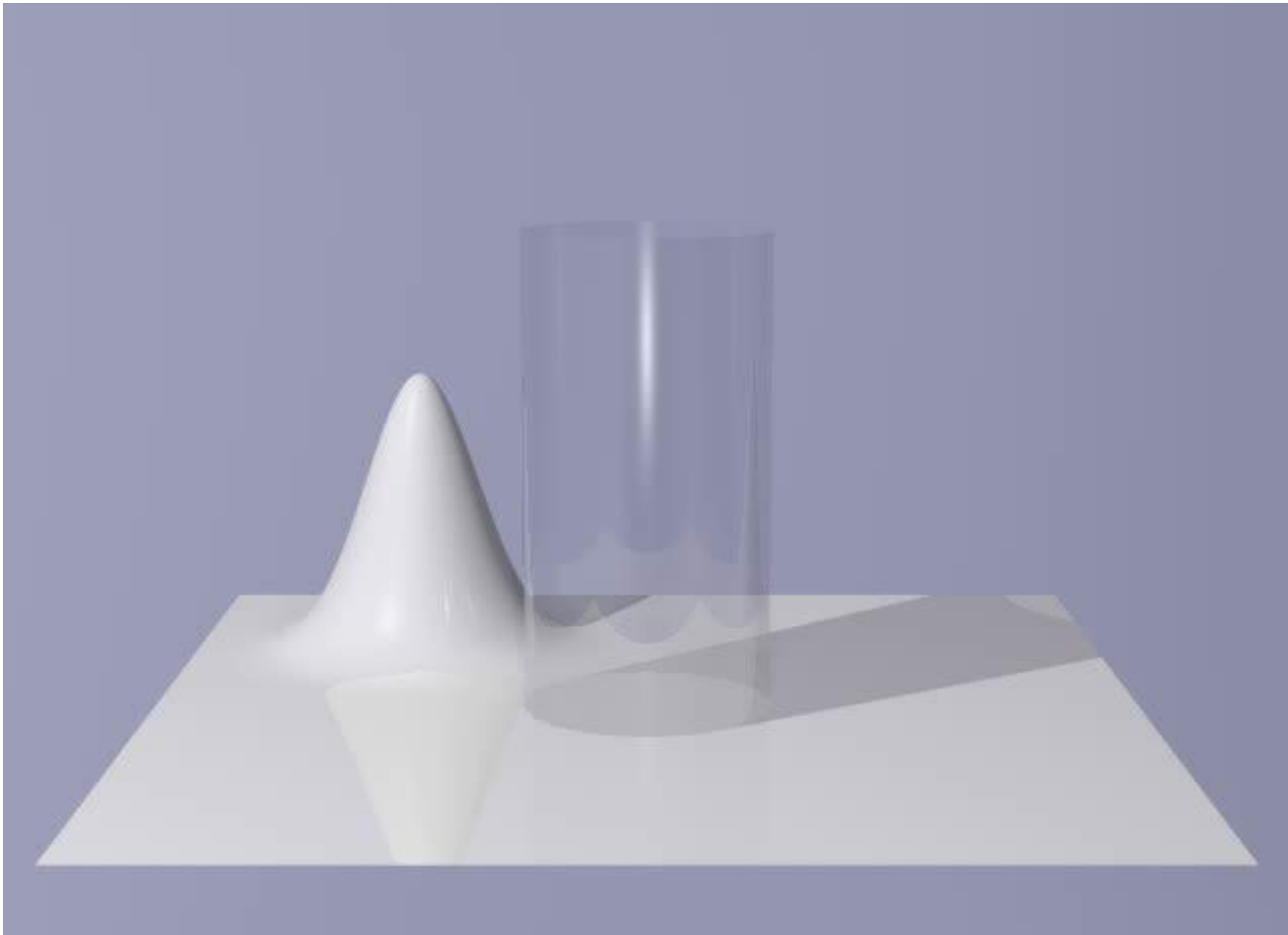
Circular barrier (Schrodinger with $\varepsilon=1/400$)



Circular barrier (semiclassical model)



Circular barrier (classical model)



Entropy

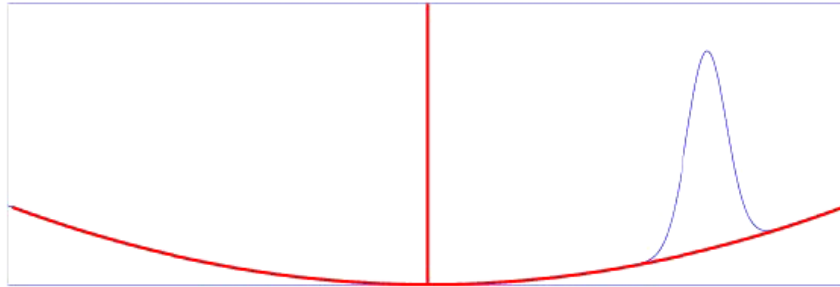
- The semiclassical model is time-irreversible.

Loss of the phase information
cannot deal with **inteference**

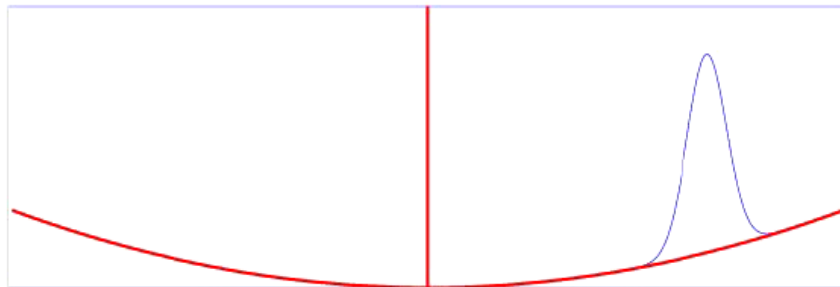
decoherence

$$V(x) = \delta(x) + x^2/2$$

Quantum



semiclassical

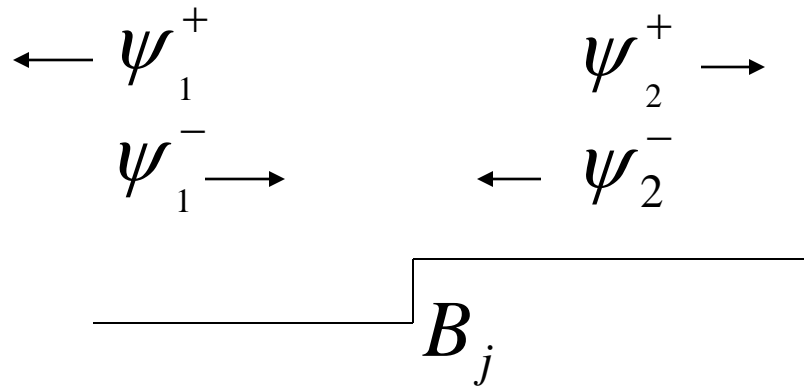


A Coherent Semiclassical Model

Initialization:

- Divide barrier into several thin barriers
- Solve stationary Schrödinger equation

$$B_1, B_2, \dots, B_n$$



- Matching conditions

$$\begin{pmatrix} \psi_1^+ \\ \psi_2^+ \end{pmatrix} = \begin{pmatrix} r_1 & t_2 \\ t_1 & r_2 \end{pmatrix} \begin{pmatrix} \psi_1^- \\ \psi_2^- \end{pmatrix} = S_j \begin{pmatrix} \psi_1^- \\ \psi_2^- \end{pmatrix}$$

A coherent model

- Initial conditions $\Phi(x, p, 0) = \sqrt{f(x, p, 0)}$

- Solve Liouville equation

$$\frac{d\Phi}{dt} = \frac{\partial\Phi}{dt} + p \frac{\partial\Phi}{dx} - \frac{dV}{dx} \frac{\partial\Phi}{dp} = 0$$

- Interface condition

$$\begin{pmatrix} \Phi_{j-1}^+ \\ \Phi_j^+ \end{pmatrix} = S_j \begin{pmatrix} \Phi_{j-1}^- \\ \Phi_j^- \end{pmatrix}$$

- Solution $f(x, p, t) = |\Phi(x, p, t)|^2$

Interference

Define the semiclassical probability amplitude as

$$\Phi(x, p, t) = \sqrt{f(x, p, t)} e^{i\theta(x, p)}$$

where $\theta(x, p)$ is the phase offset from the initial conditions $\Phi(x, p, 0) = \sqrt{f(x, p, 0)}$.

Hence, if $\Phi(x, p, t)$ is a solution to the Liouville equation for initial condition $\Phi(x, p, 0)$, then $f_{\text{coh}}(x, p, t)$ is a solution to the Liouville equation for initial condition $f_{\text{coh}}(x, p, 0)$. Furthermore, for two solutions Φ_1 and Φ_2 with $f_1 = |\Phi_1|^2$ and $f_2 = |\Phi_2|^2$,

$$|\Phi_1 + \Phi_2|^2 = f_1 + f_2 + 2\sqrt{f_1 f_2} \cos(\theta_1 - \theta_2). \quad (10)$$

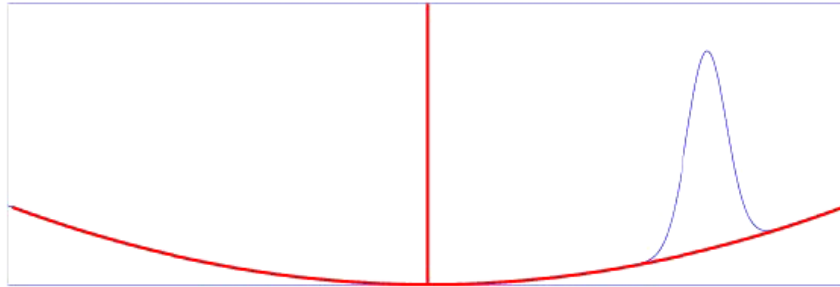
For any two probability densities ψ_1 and ψ_2 with $\rho_1 = \int f_1 dp = |\psi_1|^2$ and $\rho_2 = \int f_2 dp = |\psi_2|^2$,

$$|\psi_1 + \psi_2|^2 = \rho_1 + \rho_2 + 2\sqrt{\rho_1 \rho_2} \cos(\theta_1 - \theta_2). \quad (11)$$

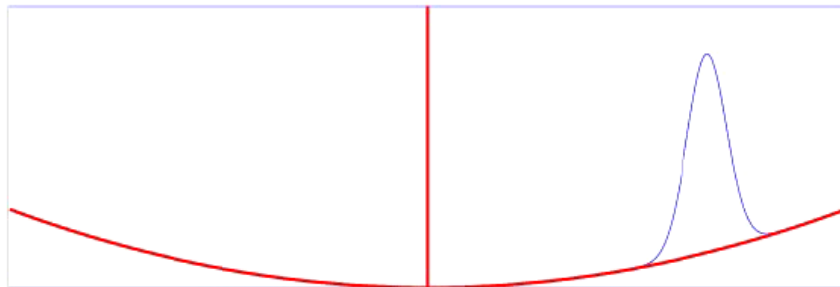
The coherent model

- $V(x) = \delta(x) + x^2/2$

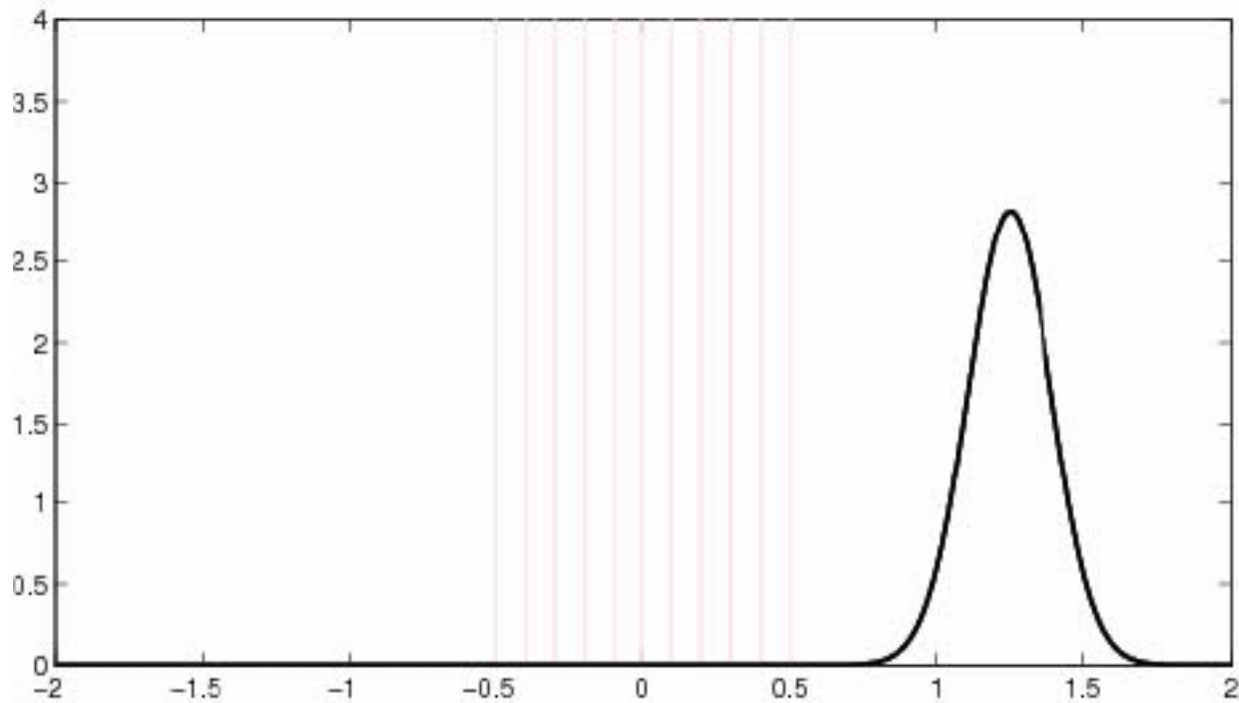
Quantum



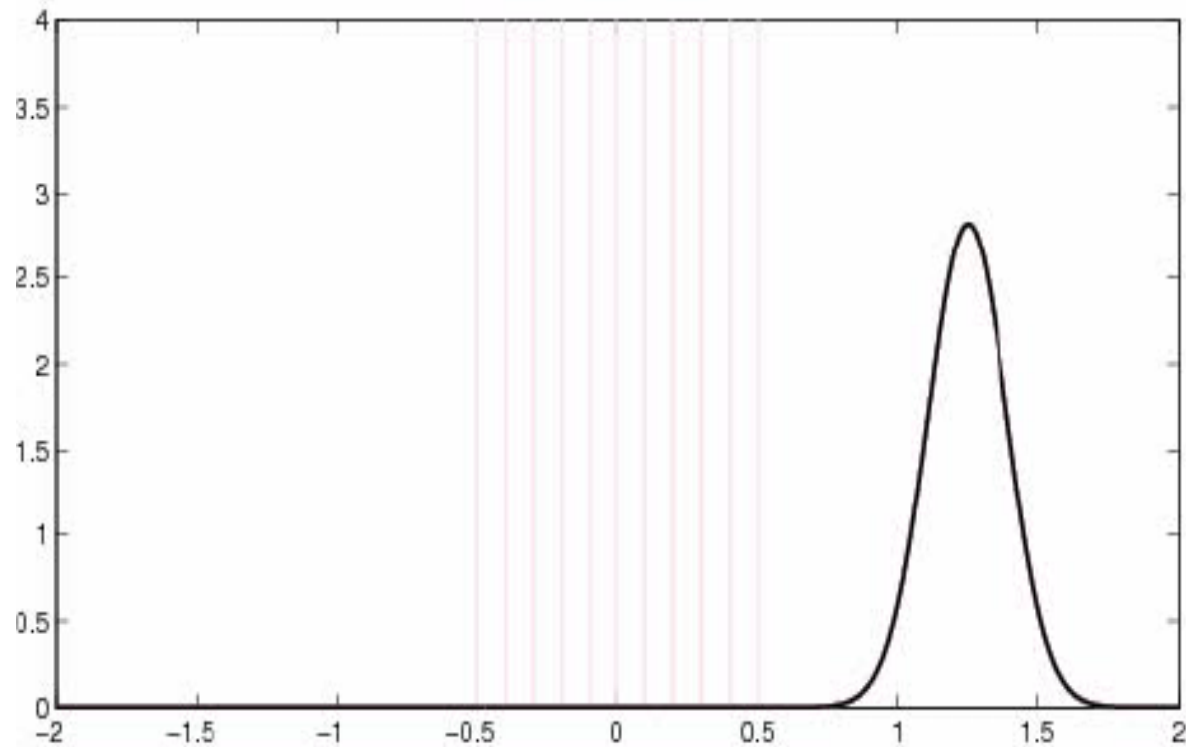
semiclassical



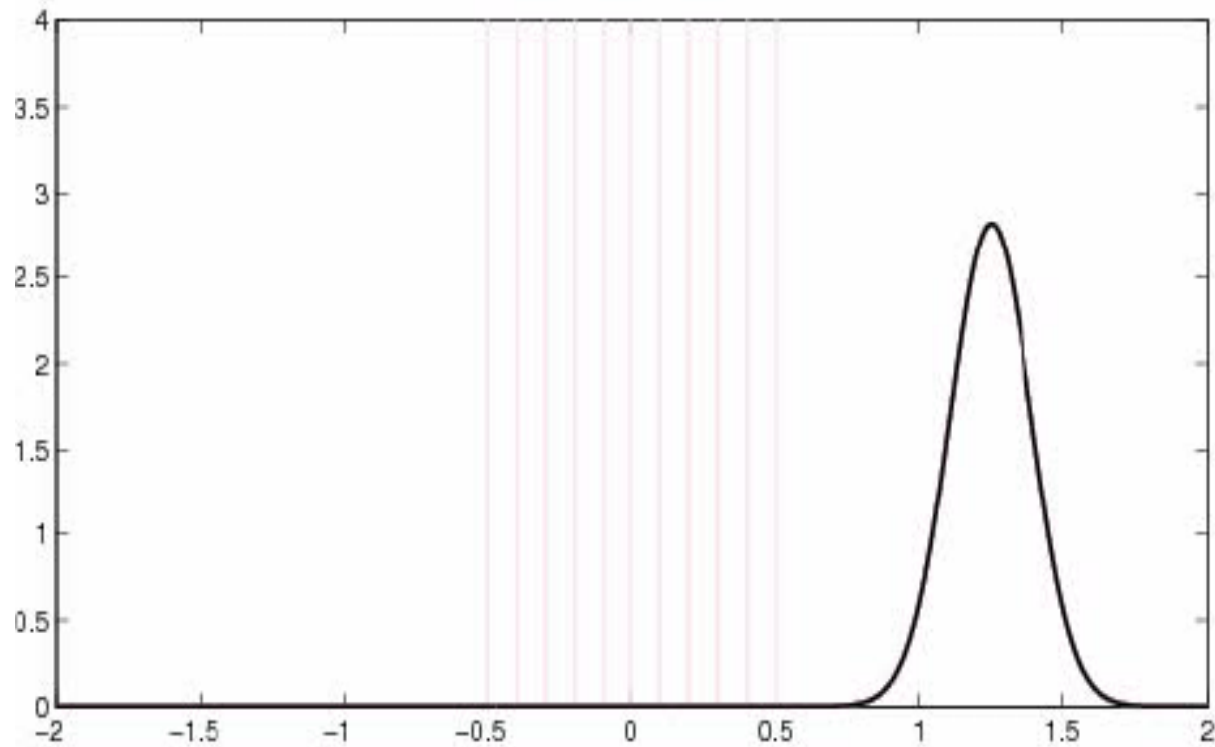
multiple delta barrier (Kronig-Penney) decoherent model vs Schrodinger



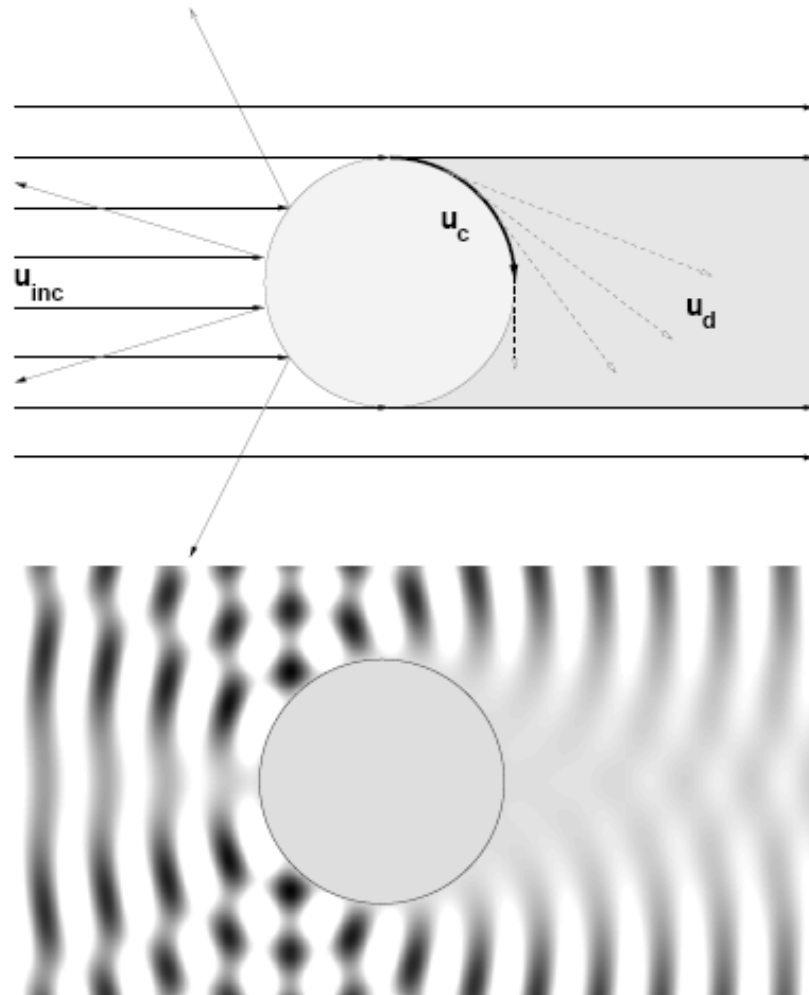
multiple delta barrier (Kronig-Penney) coherent model vs Schrodinger



multiple delta barrier (Kronig-Penney) average soln of coherent model vs Schrodinger



III. Computation of diffraction (with *Dongsheng Yin*)



Transmissions, reflections and diffractions (Type A interface)

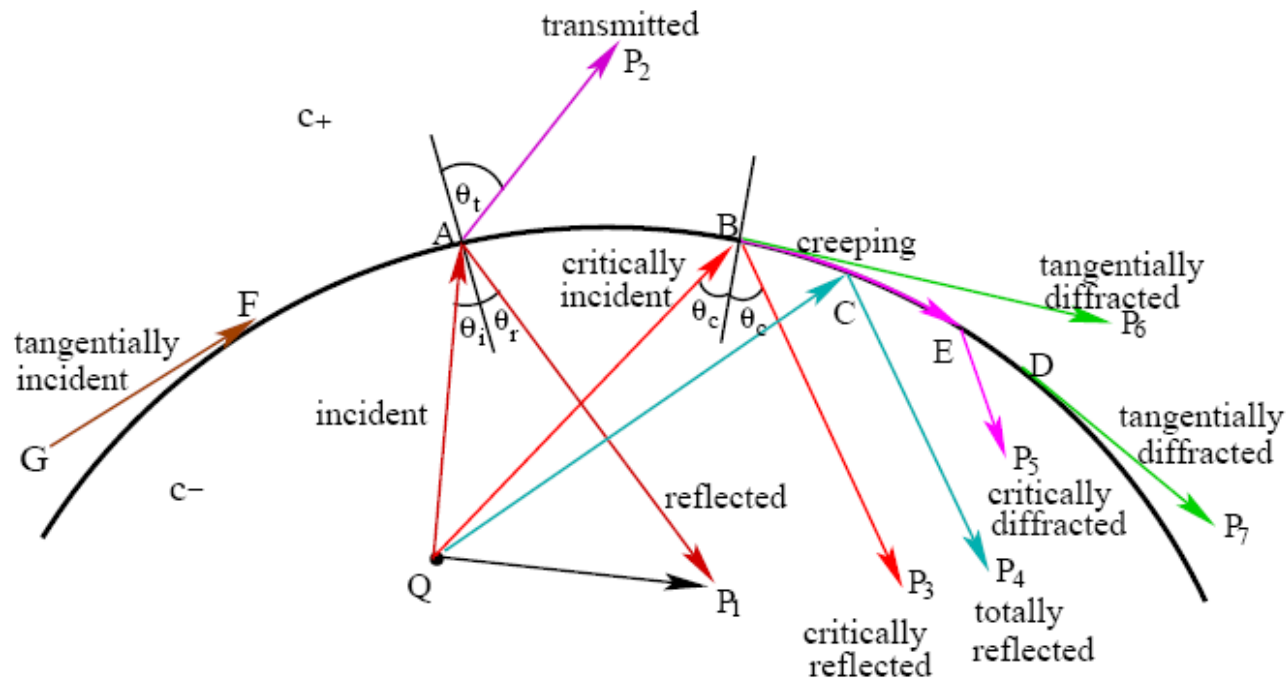


Figure 1: wave reflection, transmission and diffraction at a Type A interface

Type B interface

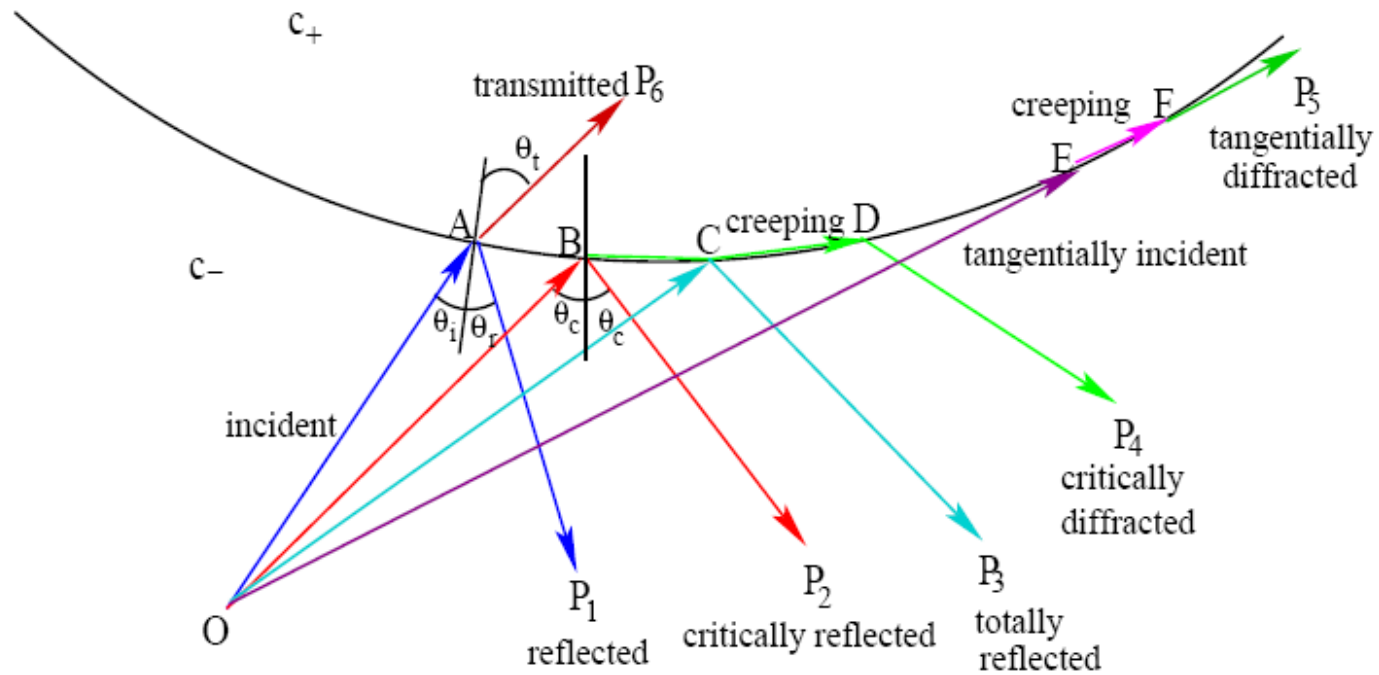


Figure 2: wave reflection, transmission and diffraction at a Type B interface

Hamiltonian preserving+Geometric Theory of Diffraction

- We uncorporate Keller's GTD theory into the interface condition:

$$\tau = \left(\frac{c^-}{c^+}\right)^2 (\xi')^2 + \left[\left(\frac{c^-}{c^+}\right)^2 - 1\right] (\eta')^2. \quad (4.1)$$

4.1 The Type B interface

We first discuss the **Type B** interface. For $\xi' > 0$, we use the following partial transmission and reflection condition at the interface:

$$f(t, \mathbf{x}^+, \xi', \eta') = \alpha_+^T f(t, \mathbf{x}^-, \xi'_t, \eta'_t) + \alpha_+^R f(t, \mathbf{x}^+, -\xi', \eta'), \quad \xi'_t > 0. \quad (4.2)$$

with $\eta'_t = \eta'$ and ξ'_t obtained from ξ' through the constant condition (1.5).

For $\xi' < 0$, there are three possibilities:

1. if $\tau > 0$ (partial reflection and transmission), then

$$f(t, \mathbf{x}^-, \xi', \eta') = \alpha_-^R f(t, \mathbf{x}^-, -\xi', \eta') + \alpha_-^T f(t, \mathbf{x}^+, \xi'_t, \eta'_t). \quad (4.3)$$

2. if $\tau < 0$ (complete reflection), the interface condition is

$$f(t, \mathbf{x}^-, \xi', \eta') = f(t, \mathbf{x}^-, -\xi', \eta'). \quad (4.4)$$

3. if $\tau = 0$ (**Case I**), there will be some diffractions, so the interface condition is

$$f(t, \mathbf{x}^-(s), \xi', \eta') = \alpha_{B_1}^D(\mathbf{x}(s)) \int_{s_b}^s \alpha_{B_1}^D(\mathbf{x}(s_q)) e^{-\int_{s_q}^s \beta_{B_1}(\mathbf{x}(z)) dz} \\ \cdot \int_{\Gamma_q} f(t - \bar{t}_q, \mathbf{x}^-(s_q), \xi'_q, \eta'(\xi'_q)) d\xi'_q ds_q + (1 - \alpha_{B_1}^D(\mathbf{x}(s))) f(t, \mathbf{x}^-(s), -\xi', \eta'), \quad (4.5)$$

here Γ_q is the *line of critical angle*

$$\frac{\xi'_q}{\eta'_q} = \text{sgn}(\eta') \sqrt{\left(\frac{c^+(\mathbf{x}(s_q))}{c^-(\mathbf{x}(s_q))}\right)^2 - 1}. \quad (4.6)$$

If $\xi' = 0$ (case **II**), there will be some tangentially diffracted waves, so

$$\begin{aligned}
f(t, \mathbf{x}^-, \xi', \eta') &= \alpha_{B_2}^D(\mathbf{x}) \int_{s_b}^s \alpha_{B_2}^D(\mathbf{x}_q) e^{-\int_{s_q}^s \beta_{B_2}(\mathbf{x}(z)) dz} \operatorname{sgn}(\eta') \int_0^{\operatorname{sgn}(\eta')\infty} f_-(t - \bar{t}_q, \mathbf{x}_q^-, 0, \eta'_q) d\eta'_q ds \\
&\quad + (1 - \alpha_{B_2}^D(\mathbf{x})) f_-(t, \mathbf{x}^-, \xi', \eta'), \tag{4.7}
\end{aligned}$$

where $\bar{t}_q = |\int_{s_q}^s \frac{dz}{c^-(z)}|$ is the average time,

$$f_-(t, \mathbf{x}, \xi', \eta') = \lim_{\omega \rightarrow 0^+} f(t, \mathbf{x} - \omega \mathbf{k}', \xi', \eta').$$

In this case, the incident wave tangentially hits the interface from the slow side. Part of the incident wave transforms into the creeping wave with coefficient $\alpha_{B_2}^D$, and part of the incident wave travels through tangentially with coefficient $1 - \alpha_{B_2}^D$.

A type A interface

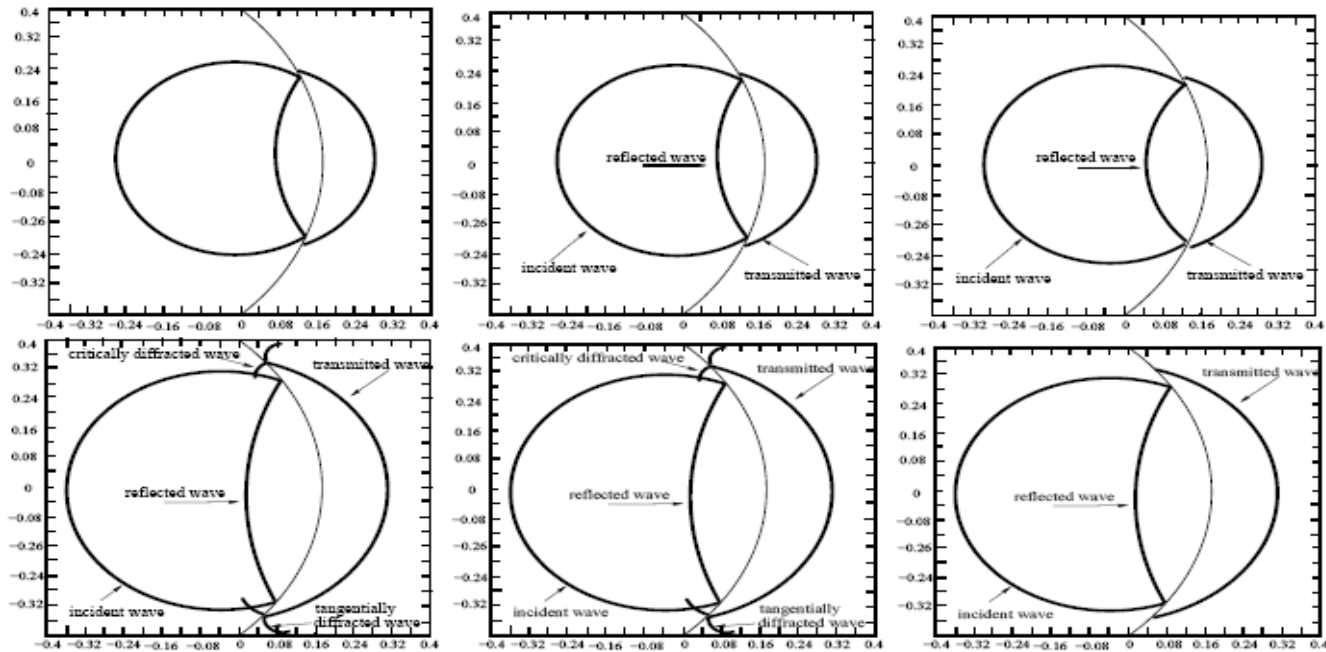


Figure 8: Example 5.3, wavefront of energy density \mathcal{E} and $\mathcal{E}^{(0)}$ at $t = 0.1$ (top) and 0.2 (bottom). Left: \mathcal{E} ; middle: $\mathcal{E}^{(0)}$ by GTD; right: $\mathcal{E}^{(0)}$ by GO.

Another type B interface

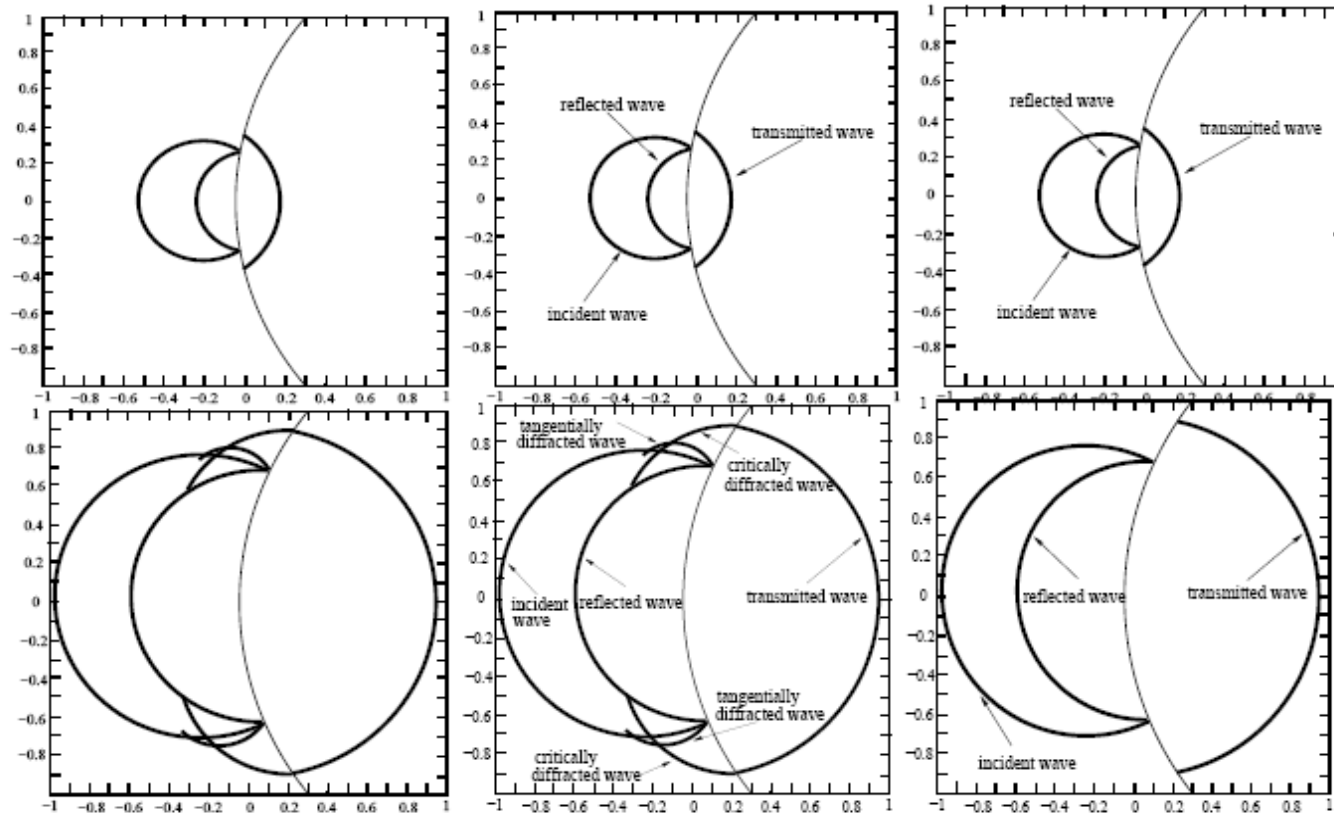


Figure 6: Example 5.2, wavefront of energy density \mathcal{E} and $\mathcal{E}^{(0)}$ at $t = 0.15$ (top) and 0.5 (bottom). Left: \mathcal{E} ; middle: $\mathcal{E}^{(0)}$ by GTD; right: $\mathcal{E}^{(0)}$ by GO.

Half plane

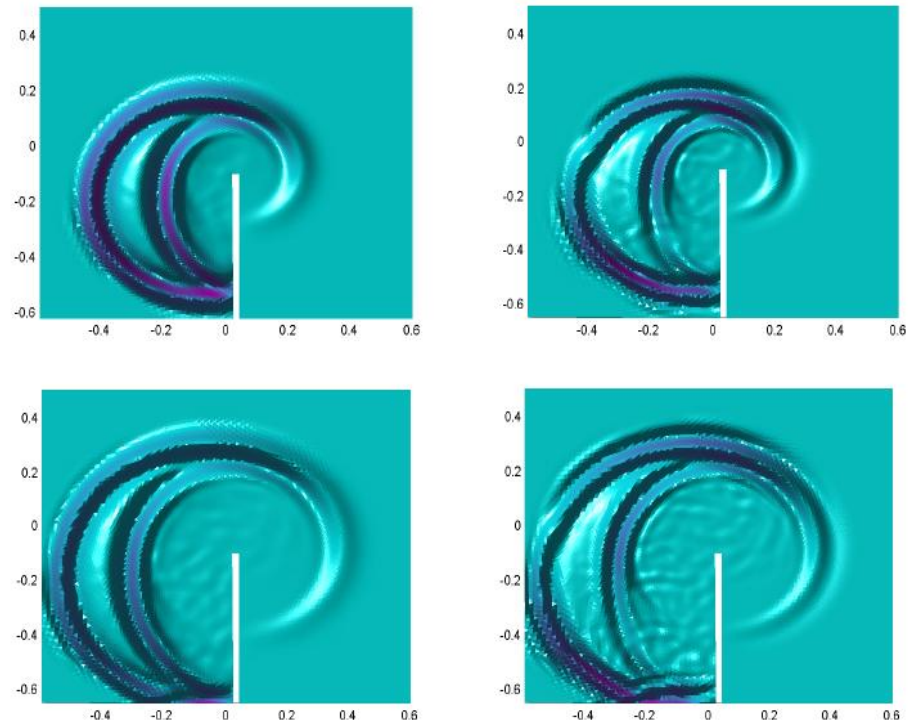
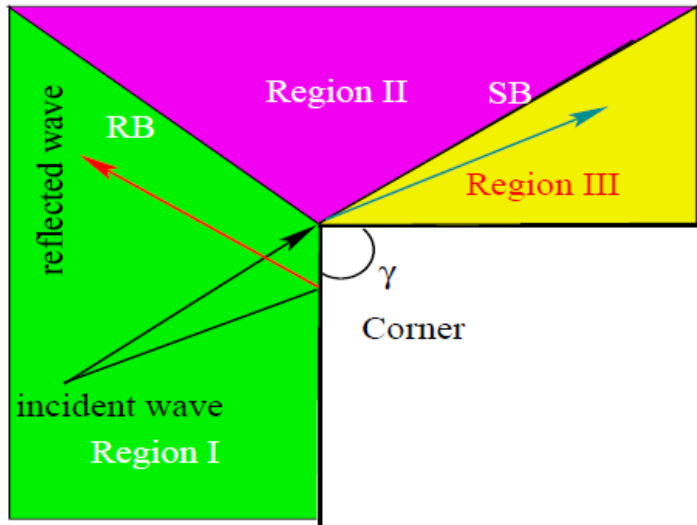


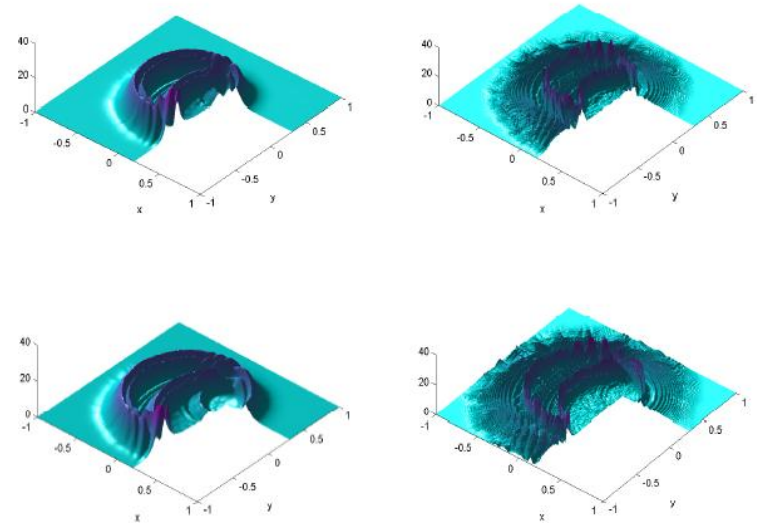
Figure 4: Example 5.1, energy density $\mathcal{E}^{(0)}$ and \mathcal{E} at $t = 0.2$ (top) and 0.3 (bottom). Left: $\mathcal{E}^{(0)}$ by GTD; right: \mathcal{E} .

Corner diffraction

Illustrative figure



GTD vs full wave simulation



VI: surface hopping (J-Qi-Zhang)

- **Born-Oppenheimer (*adiabatic*) approximation**

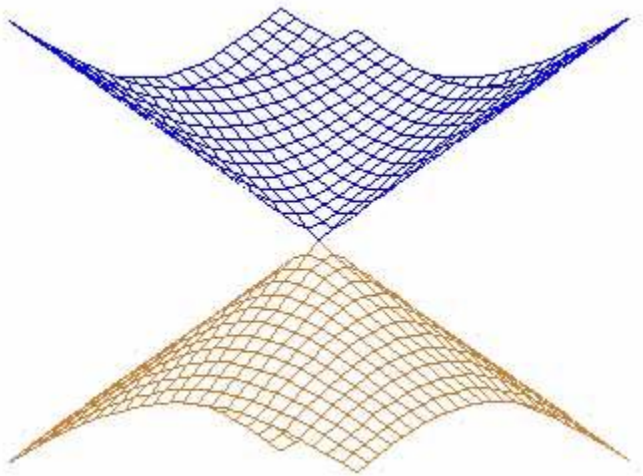
high ratio between the nuclear and electronic masses;

electronic Schrodinger equation is first solved, given electronic energy states that serve as the potential functions for the nuclear Schrodinger equation;

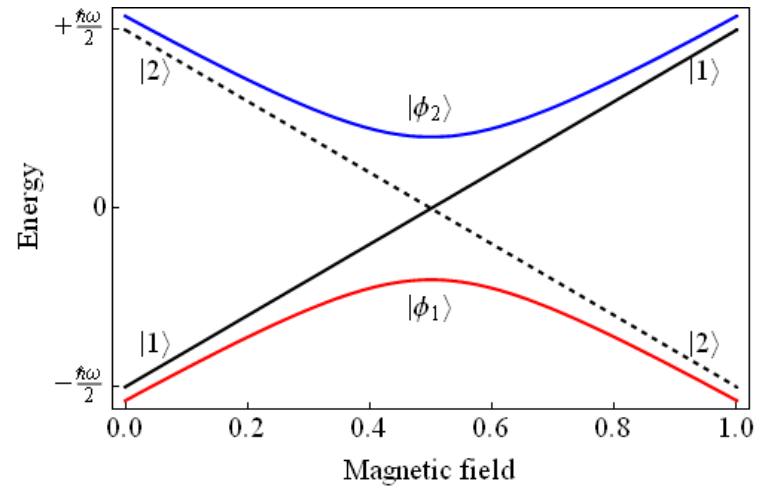
when energies of different electronic states are close , transitions between different energy states occur and the BO breakdown

Transition between electronic states

Conical crossing



Avoided crossing



The Landau-Zener formula

- gives the probability of a **diabatic** transition between the two energy states

$$P_D = e^{-2\pi\Gamma}$$
$$\Gamma = \frac{a^2/\hbar}{\left|\frac{\partial}{\partial t}(E_2 - E_1)\right|} = \frac{a^2/\hbar}{\left|\frac{dq}{dt} \frac{\partial}{\partial q}(E_2 - E_1)\right|}$$
$$= \frac{a^2}{\hbar|\alpha|}$$

The surface hopping method (Tully '71)

- Particles follow the classical trajectory determined by the classical Hamiltonian; at avoided crossing region they “hop” with transition probability to different energy level (Hamiltonian system for different potential surfaces)
- A Monte-Carlo procedure; or particle splitting

An Eulerian Surface Hopping method

- For two-energy level system we use two Liouville equations, corresponding to two Hamiltonians, with an interface condition for Landau-Zener transition

$$\partial_t u_\tau + \nabla_{\mathbf{k}} \lambda_\tau \cdot \nabla_{\mathbf{x}} u_\tau - \nabla_{\mathbf{x}} \lambda_\tau \cdot \nabla_{\mathbf{k}} u_\tau = 0, \quad (t, \mathbf{x}, \mathbf{k}) \in \mathbb{R}^+ \times \Omega, \quad \tau = 1, 2,$$

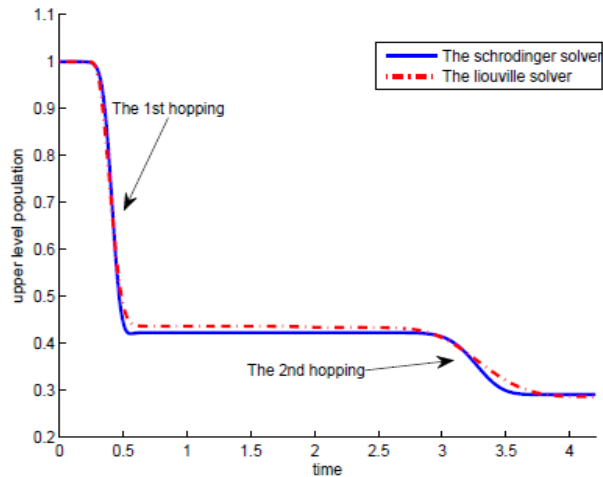
$$j_\tau(\mathbf{x}, \mathbf{k}) = \nabla_{(\mathbf{x}, \mathbf{k})} u_\tau(\mathbf{x}, \mathbf{k}), \quad \tau = 1, 2,$$

$$\begin{pmatrix} j_1(\mathbf{x}_0^+, \mathbf{k}_0^+) \cdot \vec{n} \\ j_2(\mathbf{x}_0^+, \mathbf{k}_0^+) \cdot \vec{n} \end{pmatrix} = \begin{pmatrix} 1 - T(\mathbf{x}_0, \mathbf{k}_0) & T(\mathbf{x}_0, \mathbf{k}_0) \\ T(\mathbf{x}_0, \mathbf{k}_0) & 1 - T(\mathbf{x}_0, \mathbf{k}_0) \end{pmatrix} \begin{pmatrix} j_1(\mathbf{x}_0^-, \mathbf{k}_0^-) \cdot \vec{n} \\ j_2(\mathbf{x}_0^-, \mathbf{k}_0^-) \cdot \vec{n} \end{pmatrix}$$

Numerical Examples

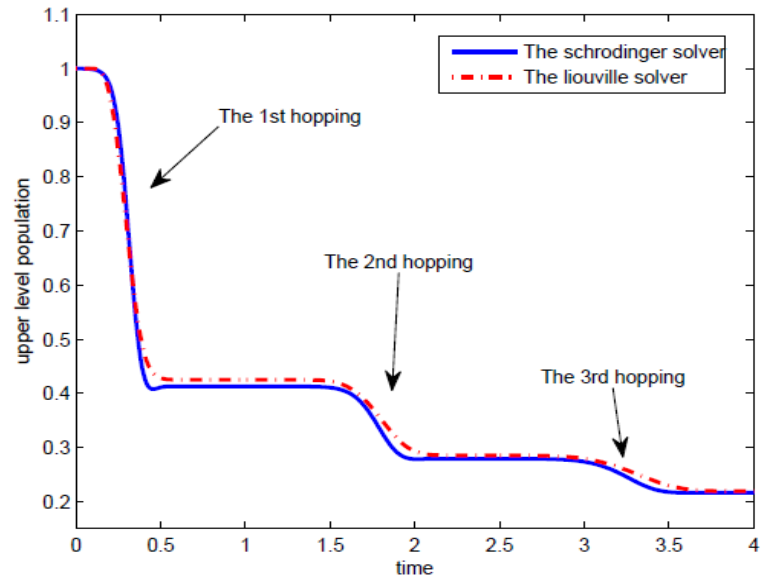
Linear isotropic potential

$$V_{iso}(\mathbf{x}) = \begin{pmatrix} x & y \\ y & -x \end{pmatrix}$$



John-Teller potential

$$V_{JT}(\mathbf{x}) = |\mathbf{x}|^2 + \begin{pmatrix} x & y \\ y & -x \end{pmatrix}$$



Advantage of Eulerian method

- No Monte-Carlo procedure
- High order accuracy
- Easily adopted to any number of energy states—
number of Liouville equations fixed
- Arise naturally from semiclassical limit of
systems of Schrodinger equation via the Wigner
transform (Spohn, Teufel, Hagedorn, Lasser,
Schutte, etc.)

V. An Eulerian Gaussian-Beam Method (J-Wu-Yang)

- Geometric optics or semiclassical limit blows up density at caustics. Gaussian beam is more accurate at caustics and preserves the Maslov-Keller phase shift

$$\varphi_{ia}^\varepsilon(t, \mathbf{x}, \mathbf{y}_0) = A(t, \mathbf{y}) e^{iT(t, \mathbf{x}, \mathbf{y})/\varepsilon}, \quad (2.1)$$

where $\mathbf{y} = \mathbf{y}(t, \mathbf{y}_0)$ and $T(t, \mathbf{x}, \mathbf{y})$ is given by the Taylor expansion

$$T(t, \mathbf{x}, \mathbf{y}) = S(t, \mathbf{y}) + \mathbf{p}(t, \mathbf{y}) \cdot (\mathbf{x} - \mathbf{y}) + \frac{1}{2} (\mathbf{x} - \mathbf{y})^\top M(t, \mathbf{y}) (\mathbf{x} - \mathbf{y}) + O(|\mathbf{x} - \mathbf{y}|^3), \quad (2.2)$$

in which $(\mathbf{x} - \mathbf{y})^\top$ is the transpose of $(\mathbf{x} - \mathbf{y})$. Here $S \in \mathbb{R}$, $\mathbf{p} \in \mathbb{R}^n$, $A \in \mathbb{C}$, $M \in \mathbb{C}^{n \times n}$. The imaginary part of M will be chosen so that (2.1) has a Gaussian beam profile. We call (2.1) as the beam-shaped ansatz.

Lagrangian formulation (Popov, Hill, Heller)

$$\begin{aligned}\frac{d\mathbf{y}}{dt} &= \mathbf{p}, \\ \frac{d\mathbf{p}}{dt} &= -\nabla_{\mathbf{x}}V, \\ \frac{dM}{dt} &= -M^2 - \nabla_{\mathbf{x}}^2V, \\ \frac{dS}{dt} &= \frac{1}{2}|\mathbf{p}|^2 - V, \\ \frac{dA}{dt} &= -\frac{1}{2}(\text{Tr}(M))A.\end{aligned}$$

$$\begin{aligned}\mathbf{y}(0, \mathbf{y}_0) &= \mathbf{y}_0, \\ \mathbf{p}(0, \mathbf{y}_0) &= \nabla_{\mathbf{x}}S_0(\mathbf{y}_0), \\ M(0, \mathbf{y}_0) &= \nabla_{\mathbf{x}}^2S_0(\mathbf{y}_0) + iI, \\ S(0, \mathbf{y}_0) &= S_0(\mathbf{y}_0), \\ A(0, \mathbf{y}_0) &= A_0(\mathbf{y}_0).\end{aligned}$$

The Lagrangian beam summation

$$\Phi_{la}^\varepsilon(t, \mathbf{x}) = \int_{\mathbb{R}^n} \left(\frac{1}{2\pi\varepsilon} \right)^{\frac{n}{2}} r_\theta(\mathbf{x} - \mathbf{y}(t, \mathbf{y}_0)) \varphi_{la}^\varepsilon(t, \mathbf{x}, \mathbf{y}_0) d\mathbf{y}_0. \quad (2.28)$$

The discrete form of (2.28) in a bounded domain is given by

$$\Phi_{la}^\varepsilon(t, \mathbf{x}) = \sum_{j=1}^{N_{\mathbf{y}_0}} \left(\frac{1}{2\pi\varepsilon} \right)^{\frac{n}{2}} r_\theta(\mathbf{x} - \mathbf{y}(t, \mathbf{y}_0^j)) \varphi_{la}^\varepsilon(t, \mathbf{x}, \mathbf{y}_0^j) \Delta \mathbf{y}_0, \quad (2.29)$$

The Eulrian formulation

$$\mathbf{L} f = \partial_t f + \xi \cdot \nabla_y f - \nabla_y V \cdot \nabla_\xi f$$

- For velocity or phase:

$$\text{Solve } \mathbf{L} \phi = 0 \quad \phi \in \mathbf{C}^n$$

$$\text{with } \phi(0, y, \xi) = -i y + (\xi - \nabla_y S_0)$$

$$\text{(note } \text{Re}(\phi) = 0 \text{ at } \xi = u = \nabla_y S)$$

- For Hessian: $M = -\nabla_y \phi (\nabla_\xi \phi)^{-1}$

- For amplitude: Solves $\mathbf{L} \psi = 0$, $\psi \in \mathbf{R}$

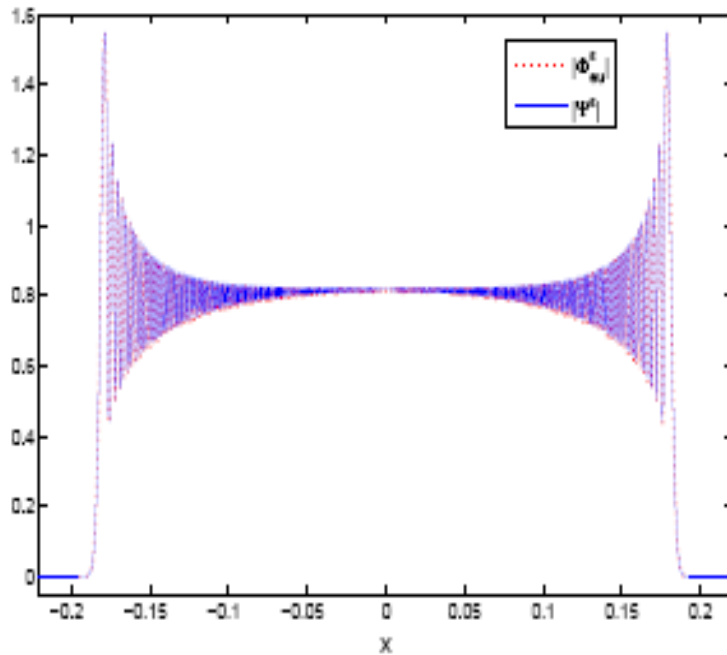
$$\text{with } \psi(0, y, \xi) = |A_0|^2$$

$$\text{then } A(t, x) = (\det (\nabla_\xi \phi)^{-1}) \psi^{1/2} \text{ (principle value)}$$

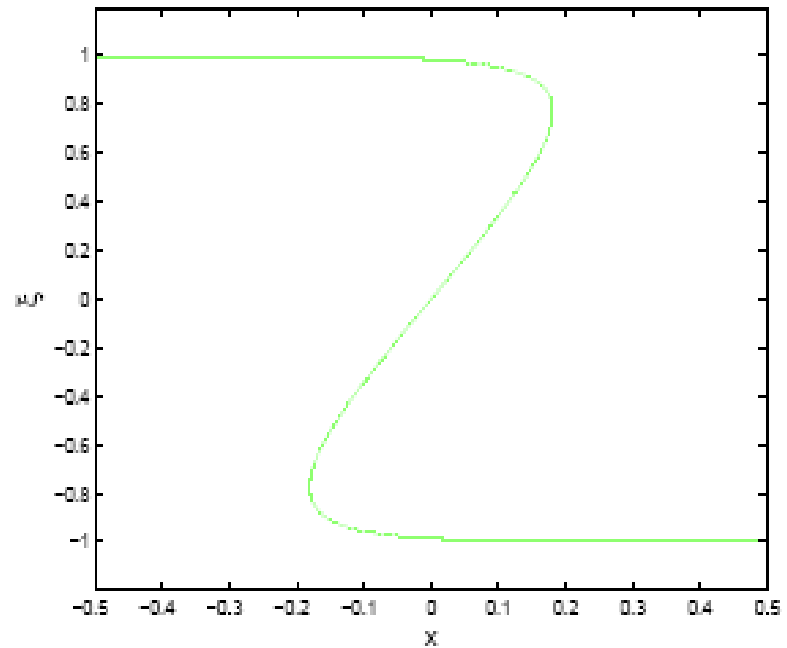
The complexity is comparable to geometric optics or semiclassical limit;
only now that $\phi \in \mathbf{C}^n$ rather than \mathbf{R}^n

A numerical example ($\varepsilon=10^{-4}$)

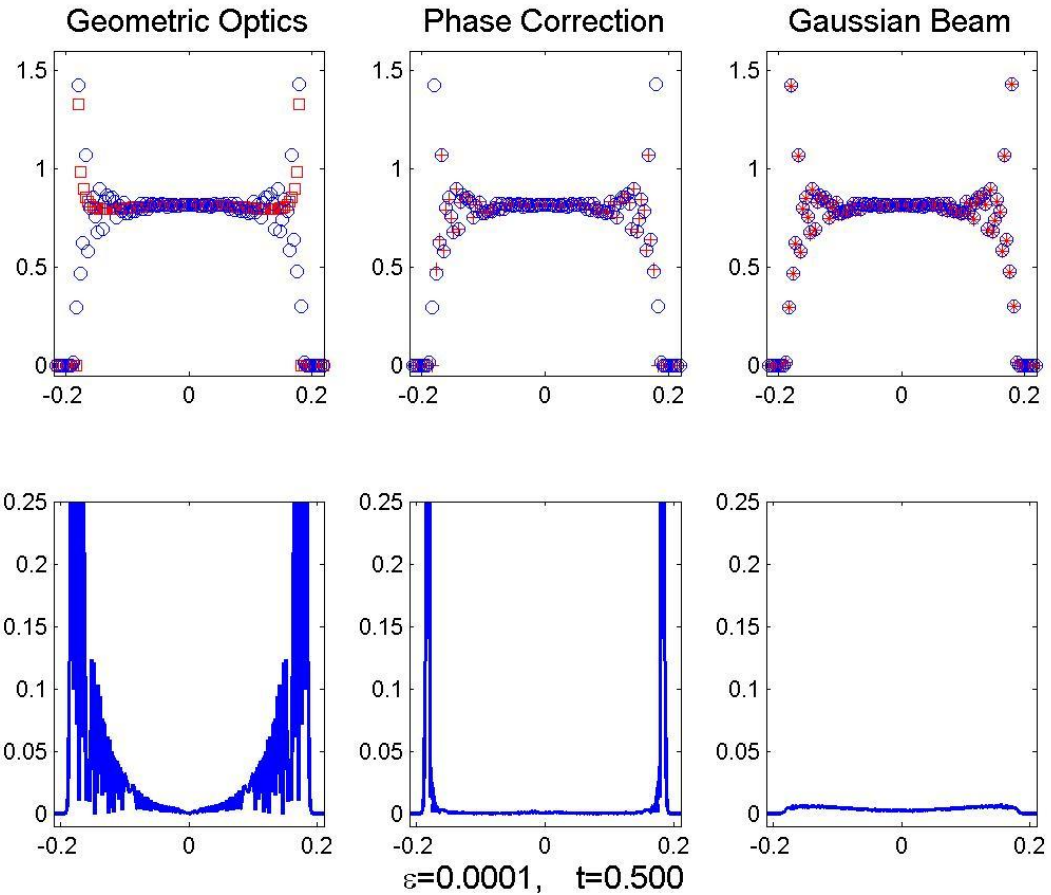
- Density



- Velocity



Error comparison



Summary

Liouville equation based Eulerian computational methods for quantum dynamics:

- Partial transmissions and reflections, diffractions, and quantum barriers
- Surface hopping
- Gaussian beam methods as an improvement of the classical solver
- Computational cost is classical, yet certain important quantum information are captured
- can use local level set method to further reduce the cost

Future projects

- Gaussian beam for interface and quantum barriers
- Coherent semiclassical models for multi-D quantum barriers
- Gaussian beam or coherent quantum-classical coupling for surface hopping

Computational cost ($\varepsilon=10^{-6}$)

- Full simulation of original problem for
 $\Delta x \sim \Delta t \sim O(\varepsilon)=O(10^{-6})$

Dimension total cost

2d, $O(10^{18})$

3d $O(10^{24})$

- Liouville based solver for diffraction

$$\Delta x \sim \Delta t \sim O(\varepsilon^{1/3}) = O(10^{-2})$$

Dimension total cost

2d, $O(10^{10})$

3d $O(10^{14})$

Can be much less with local mesh refinement